INTERNATIONAL JOURNAL OF COMPUTER ENGINEERING &TECHNOLOGY (IJCET)

ISSN Print: 0976-6367
ISSN Online: 0976-6375

Publishers of High Quality Peer Reviewed Refereed Scientific, Engineering & Technology, Medicine and Management International Journals

PUBLISHED BY

IAEME

IAEME Publication

Chennai, India

https://iaeme.com/Home/journal/IJCET

International Journal of Computer Engineering and Technology (IJCET)
Volume 16, Issue 3, May-June 2025, pp. 607-635, Article ID: IJCET_16_03_037
Available online at https://iaeme.com/Home/issue/IJCET?Volume=16&Issue=3
ISSN Print: 0976-6367; ISSN Online: 0976-6375; Journal ID: 5751-5249
Impact Factor (2025): 18.59 (Based on Google Scholar Citation)
DOI: https://doi.org/10.34218/IJCET_16_03_037

LEUKEMIA CLASSIFICATION USING AN OPTIMIZED HYBRID MODEL: CNN, RESNET, DNN, AND XGBOOST IN PERSPECTIVE

Lila Misra[*1], Dr.Rahul Shrivastava[2]

[*1]Department of Computer Science, Mansarovar Global University, Sehore, MP, India
[2]Department of Computer Science, Mansarovar Global University, Sehore, MP, India.

***Corresponding Author: Lila Misra**

ABSTRACT

Leukemia is a fatal cancer affecting individuals of all ages, primarily involving abnormal increases in immature white blood cells that impair bone marrow and blood function. Accurate and timely diagnosis is essential but current manual microscopic analysis is slow, error-prone, and challenged by the similarity between healthy and leukemic cells. This study proposes a novel Federated Learning (FL)-based Deep Learning (DL) framework for leukemia detection, ensuring privacy-preserving training across distributed clients. Input images are first denoised using an Adaptive Median Filter (AMF), followed by Scribble2label-based cell segmentation and image augmentation. Features are then extracted and classified using a Dense Convolutional Network (DenseNet), optimized through a proposed Fractional Mayfly Optimization (FMO) method, which integrates the Mayfly Algorithm and Fractional Calculus. Local model updates are aggregated at the server via RV coefficient-weighted averaging. The

proposed FMO-DenseNet achieves high performance with 94.3% accuracy, 5.7% loss, 9.2% MSE, 0.965 TNR, and 0.953 TPR.

Keywords: fractional Calculus, DCNN, Leukemia; federated learning, fractional concept; May-fly Algorithm.

Cite this Article: Lila Misra, Rahul Shrivastava. (2025). Leukemia Classification Using an Optimized Hybrid Model: CNN, Resnet, DNN, And XGBOOST in Perspective. *International Journal of Computer Engineering and Technology (IJCET)*, 16(3), 607–635.

https://iaeme.com/MasterAdmin/Journal_uploads/IJCET/VOLUME_16_ISSUE_3/IJCET_16_03_037.pdf

1. Introduction

Cancer occurs due to the fast-developing cells that grow beyond their normal boundaries. It affects body parts and spreads to other organs. This condition is known as cancer. Leukemia is the other name for blood cancer. The Greek words "leukos" which means "white" and "aim" which means "blood," are used in the entomology of leukemia.[28] There is an uncontrollable excess or morphological disruption of leucocytes in the blood due to malignancy developing in the bone marrow. [5] The basic method of classifying leukemia depends on whether it is acute or chronic and whether it originates in lymphoid or myeloid cells. Knowing the precise type of leukemia helps medical professionals better determine each prognosis of the patient and choose the most effective treatment. [3] Identification of leukemia is essential since it has a significant impact on prognosis and immediate therapy results. Despite the fact that it is well known that automated blood cell images, analyzers typically under estimate the quantity of blast cells. [29][2] For early and reliable identification, the manual recognition of this malignancy necessitates a skilled doctor or physician. It is a common procedure to examine blood smear images to find Acute Lymphoblastic Leukemia (ALL). However, due to the complexity of blood cells and the reliance on human interpretation, manual identification is complicated by difficulties including noise, blur, weak edges, and weak edges.[6]

Leukemia can be categorized based on the malignant cell type, such as lymphoid or myeloid, and based on the rate of symptom development such as chronic or acute. ALL is most prevalent in children and due to genetic causes, the Hispanic population is most impacted by ALL globally. A formation of morphological and molecular principle is currently used to diagnose leukemia. The morphological classification is based on the medical norms, which were created to recognize the traits, like number of white blood cells, form, and size, to

determine the possibility of distinguishing the categories. The time required for the analysis of each sample by the expert and the accuracy of the diagnosis are two significant drawbacks of this process. [30] Medical professionals are helped by Computer-Aided Diagnostic (CAD) systems to do everyday tasks more quickly, accurately, and efficiently. [8] Hematologists frequently employ a variety of invasive techniques to diagnose the condition. An invasive procedure called biopsy typically involves examining spinal fluid, bone marrow, or blood, and it is used to diagnose most cases. These procedures are difficult, expensive, and timeconsuming. The doctor performing these examinations checks for signs of ALL, which are extremely likely to be present if the number of WBCs is high enough and there are other pertinent physical observations. [1] FL has been suggested as an alternate environment, in which a common global model is tuned from federation of contributing devices under the direction of a fundamental server. The participating devices (clients) are often many and their internet connections are inconsistent or slow. When training data is derived from user interactions with mobile applications, it serves as a major motivator for FL. It separates the capability of Machine Learning (ML) from requirement for data storage in the cloud by allowing mobile devices to supportively establish a shared prediction model while keeping all the training data on the device. Mobile devices are used by users as nodes to process local data so as to update a global model and training data is stored locally. Furthermore, local models that are used to make predictions on mobile devices, this also brings model training to device. The huge amount of clients, the very unstable and non-i.i.d. data available on each client, and the often- poor network connections set the system above apart from standard distributed ML. [27] Advances in ML and Deep Learning (DL) can assist in more correctly detecting the disease as well as assisting medical professionals in appropriately diagnosing and treating the disease. [31] The process chosen comprises image preprocessing, feature extraction, feature selection, and classification. [6] Using two-dimensional convolutional filters, a Deep Neural Network (DNN) may mechanically mined task-specific features to get around the issue of predetermined features. DNN are frequently used in computer vision, particularly for medical image analysis include disease classification, detection, [32] registration, localization, and segmentation. 1 The server and the nodes are the two entities elaborate in the FL process. In this context, local training is carried out at each node using local data. Moreover, model aggregation is performed at the server and global model is then downloaded at nodes. Additionally, training is updated using both transferred global model and local model. The objective is to develop a system of classification for leukemia utilizing the proposed FMO-DenseNet. The initial step is the

acquisition of input image from given dataset and the image is sent to pre-processing. An AMF is used for pre-processing. After completion of image pre-processing, data augmentation is performed, and then extraction of feature is effectuated. The classification of leukemia is then performed using DenseNet, which is tuned by proposed FMO. Here, FMO is a novel approach formed by fusing MA and FC. The core contributions of this work include the following:

Developed FMO-DenseNet for leukemia classification: A new optimization-driven model, called FMO-DenseNet is formed to classify leukemia in a FL framework. Leukemia classification is accomplished by using DenseNet, which is tuned based on proposed FMO. Here, FMO is newly formulated by the formation of FC and MA.

1.1 Literature survey

Zakir Ullah, M., et al. [1] developed CNN for the classification of ALL cancer. Here, this technique was easier and produced acceptable outcomes for the ALL diagnosis. It was also utilized by pathologists as a supplementary diagnostic tool. However, it neglected to consider multi-class categorization and many data datasets of the same or related diseases to improve the efficacy.

Ansari, S., et al. [2] introduced the DL model for the diagnosis of acute leukemia cells. The time-consuming issue of selecting the features was resolved by this technipque. Nevertheless, it failed to evaluate relevant research in real-time applications and contemplate more image classification scenarios.

Ramaneswaran, S., et al. [3] established hybrid inception v3 XGBoost model for ALL classification. In this case, the approach was made easier without affecting efficiency by using a single Convolutional Neural Network (CNN) backbone. However, this approach failed to create a synthetic dataset with Generative Adversarial Network (GAN) to advance research. Sampathila,

N., et al. [4] devised anintelligent deep learning algorithm to predict the leukemic cells from the healthy blood cells. This technique was helpful during the screening process because it decreased the computing time and error rate. However, it was challenging to address the issue by expanding the database with noisy images for prediction.

Baig, R., et al. [5] developed a hybrid CNN and bagging ensemble for the diagnosis of ALL. This method reduced the implementation time of model so as to enhance its performance. However, this method failed to identify the subtype of leukemia and it did not reduce computational complexity.

Sulaiman,A., et al. [6] established ResRandSVM for the detection of ALL in blood smear images. In this case, it improved the capacities for generalization,interpretability, and

overall performance. However, additional DL and ML algorithm combinations were not considered for accuracy.

Mallick, P.K., et al. [7] introduced a DNN classifier to classify the leukemia types. The automatic analysis of microarray data was made possible by this ML technique. However, this method did not consider improving the network structure to enhance the classification.

Diaz Resendiz, J.L., et al. [8] established Residual Network-50 (ResNet-50) for the classification of ALL. This model was able to extract excellent deep features that improved classification. However, it required labeling images, which was time-consuming and prone to errors.

1.3 Challenges

Some of the complications faced by prevailing classification approaches of leukemia are listed as below:

1. An effective approach named CNN was introduced in [1] for ALL cancer classification. Here, this model achieved promising performance in terms of robustness, classification accuracy, and flexibility. However, this technique was not validated with different database of similar diseases and multi-class classifications.

2. For the purpose of ALL classification, inception v3 XGBoost was developed in. [3] This approach did not consider the usage of attention maps to make the technique more interpretable to enhance the confidence of medical practitioners.

3. In, [7] a DNN classifier was established for the purpose of leukemia classification. Here, this classifier produced an enhanced classification accuracy with minimal time consumption. In this technique, no optimization was considered to improve the detection process, which remained a challenge.

4. ResNet-50 was developed in [8] for diagnosing leukemia disease. In this case, this model significantly improved model consistency, interpretability, and visualclarification. Nevertheless, it failed to consider numerous types of WBC to produce a more powerful ensemble classifier for increasing the accuracy of classification.

5. All the above-mentioned difficulties can limit the overall performance. Hence, there is still a need to develop high-performance systems on the basis of larger datasets. Existing approaches struggle to explain the underlying logic behind modelpredictions and to be robust

2. Materials

2.1 Experimental set-up

The experimental setup of FMO-DenseNet is executed utilizing PYTHON tool.

2.2 Description about dataset

The complete analysis of ALL,[26] as a highly predominant cancer, necessitates expensive, invasive, and time-consuming diagnostic tests. utilizing Peripheral Blood Smear (PBS) images for ALL diagnosis is a crucial step in the early differentiation of cancer cases from non-cancer cases. The bone marrow laboratory at Taleqani Hospital (Tehran, Iran) prepared images for this dataset. This database comprised of PBS images from 89 individuals assumed of having ALL, whose blood samples had been processed and marked by qualified laboratory staff. The classes benign and malignant in this database are separated. A Zeiss camera set at a 100x magnification was used to capture each image, which was then saved as a JPG file.

2.3 leukemia classification [Federated learning]

FL23 is an evolving distributed collaborative AI framework, and it is most commonly used for smart healthcare. Here, the training of AI is performed without sharing data by coordinating multiple clients like hospitals. Therefore, a novel optimization-based DL technique using FL is proposed in this research. In FL, different entities are considered including servers and nodes. Every node does local training on the basis of local data, and the server receives updated weights for the model aggregate. Then, the global model is downloaded at every node, and training process is carried out at each node iteratively utilizing the local model and downloaded global model. The block diagram of FL for classifying leukemia is shown in Figure 1.

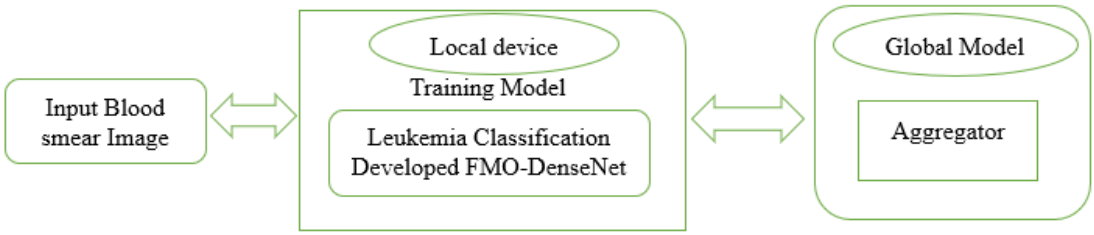

2.3.1 Local training based on local data

FL enables two participants to collaborate and train DL in a decentralized manner. Each FL user creates a method locally utilizing information from their own device, then uploads the

ideas of the model to a centralized server that gathers updates from all devices. Once a certain number of devices have generated their updates, local training is done, and the devices are then granted access to the aggregated scheme parameters. 23

2.3.1.1 Training at every node

Each local device node obtains an image as input and initiates the training process inside the training model at a time interval t . The model or global server gathers all local device updates, and aggregates it to generate a global model. The further sections allocate a detailed description of training method utilized in the training model.

2.3.1.2 Proposed Model FMO-DenseNet for Leukemia Classification

The input image is contemplated as the input for the classification of leukemia and it is subjected to image preprocessing. AMF9 is used to eliminate noises from the input image. In order to distinguish the cells from the background, cell segmentation is then done using theScribble2label. 10 Additionally, image augmentation is used to augment number of training examples. Image augmentation is accomplished using procedures like rotation, color augmentation, scaling, and flipping. After that, feature extraction is executed, where statistical features, 12 including mean, median, standard deviation, variance, skewness, and kurtosis, CNN features, 13 GLCM features such as contrast, correlation, energy, homogeneity, and entropy, CLBP features, 15 DWT, PHOG, 16 LVP, 17 and LGXP18 are extracted. Lastly, leukemia classification is accomplished utilizing DenseNet, 19 which is trained using the proposed FMO. Here, the FMO is devised by merging MA20 and FC. 21 Following local training, the server performs local updating and aggregation using a weighted average by RV coefficient. 22 Figure 2 depicts a visual depiction of FMO-DenseNet for the classification of leukemia.

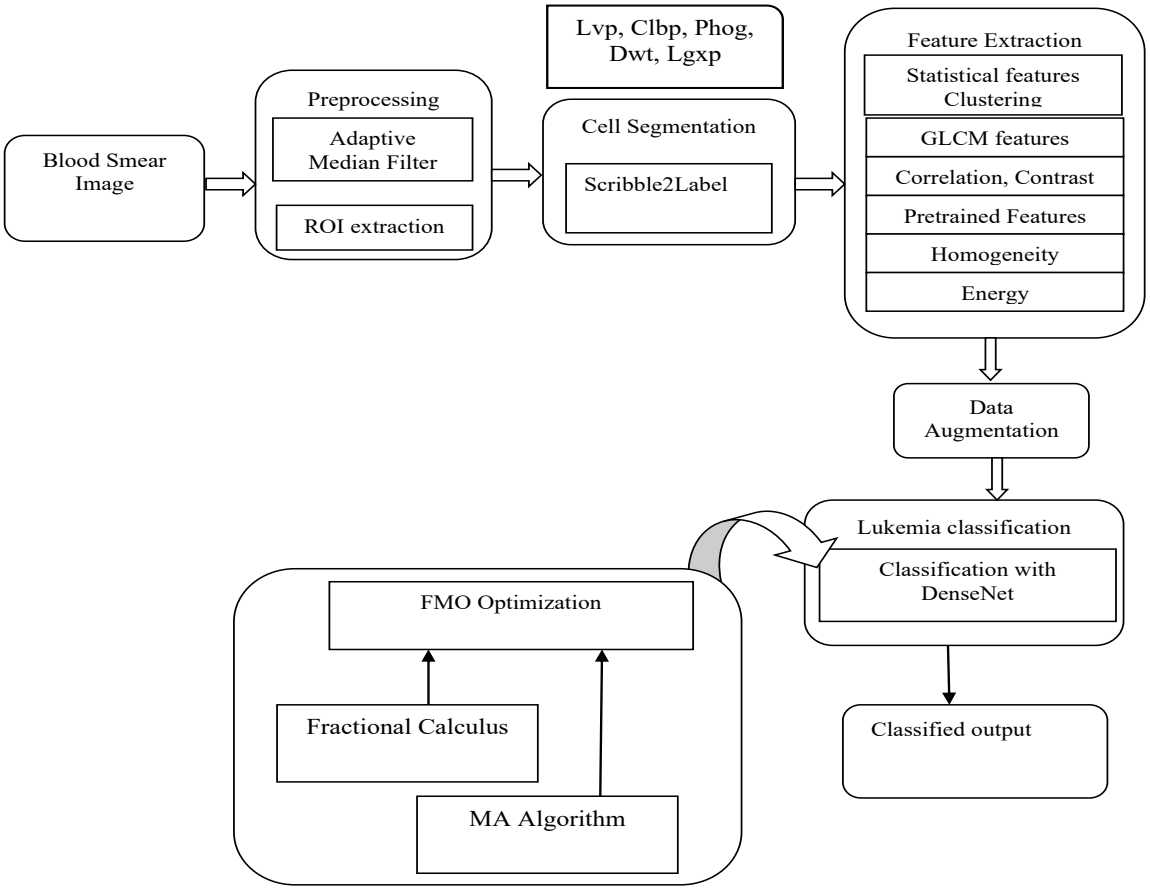

Figure2. Pictorial representation of FMO-Dense Net for classification of leukemia

a). Image acquisition

The input blood smear image is obtained from database K , which contains s images. The database is designated as below,

$$K = \{M_1, M_2, ..., M_p, ..., M_s\} \quad (1)$$

From the equation, a total number of images is characterized as s and M p denotes th p image that is used for leukemia classification.

b). Image pre-processing

Extracting the noise in the input image requires using an image pre-processing approach. The image obtained from database has some inherent noise that has to be removed. In this case, to ignore the noise component, the AMF9 is utilized. The input considered for pre-processing step is the blood smear image Mp .

Adaptive median filter

The AMF9 is employed for denoising the image Mp , and here, spatial processing is used to identify pixels in the image that are impacted by impulse noise. Each pixel in an image is compared to its neighbors to determine whether it is noise or not. Additionally, it can change the reference threshold and size of the neighborhood. Noise is defined as a pixel that is out of alignment with the majority of its neighbors and not positioned next to the pixels to which it is identical. The median pixel value from the area that passed the noise identification test is then used to replace the pixels affected by impulse noise. The AMF is effectual in minimizing distortion, eliminate impulse noise and reduction of background noise. The output attained from AMF is signified by M n

c). Cell dissection[Scribble2Label]

The pre-processed image M n is utilized as the input to the cell segmentation process. In this case, leukocytes are isolated from segments of image in order to predict specific features. Additionally, Scribble2Label is utilized to segment the cells during processing. 10 In this case, specified scribbles are represented by labeled pixels while the remaining pixels are left unlabeled. A standard cross-entropy loss is employed for the labeled or scribbled pixels. For unlabeled or unscribbled pixels, the network automatically produces suitable labels by applying an exponential moving average produced during training. There are two stages to training this model. The model is trained using simply the scribbling pixel loss in the initialization step, which is considered as a warm-up stage. Following the first model training during the warm-up step, an estimation is repeatedly refined by both scribbled and unscribbled losses.

warm-up stage: Consider the small group of user-created scribbles used as input training data. The model is only trained using the provided scribbles during the warm-up phase, producing average predictions. In this case, a subset of consistent mask annotation is represented by given scribbles. This system is cross-entropy loss trained by ignoring unscribbled pixels as described below:

$$J_{fy}(\mathrm{M}_p, f) = -\frac{1}{|\chi_f|}\sum_{N\in\chi_f}\left[f_N \log(\gamma(d;\theta_\tau)) + (1-f_N)\log(1-\gamma(d;\theta_\tau))\right] \quad (2)$$

Here, scribble annotation specified as f , set of scribbled pixels is denoted as χ_f , γ (d ; θ_τ) signifies prediction of model at iteration τ , input image represented as Mp , network is represented as θ_τ . The output attained from cell segmentation is signified as Ms .

d). Image augmentation

The segmented image M s is applied as input for image augmentation. Image augmentation[11] lessens the need for memory usage while assisting in the growth of the size of the database. It is a synthetic technique for boosting the number of training examples using duplicates of datasets built with actual data. In addition, data augmentation reduces overfitting issues. Techniques used for augmentation include rotating, scaling, flipping, and color augmentation.

i). Flipping:For the image to be reflected along either its horizontal or vertical axes or both, flipping is required. Without utilizing artificial computation, operators can raise the number of images in a dataset.

Vertical flipping: The top and bottom of the upside-down image determine the y and x axis. Here, coordinates for each pixel at moment the vertical axis flipping are represented by $h\varpi$ and h_L . It is represented as,

$$\begin{bmatrix} \hbar_{\varpi} \\ \hbar_L \end{bmatrix} = \begin{bmatrix} 1 & 0 \\ 0 & -1 \end{bmatrix} \cdot \begin{bmatrix} \varpi \\ L \end{bmatrix} \tag{3}$$

Here, the pair of coordinates is signified as ϖ and L .

Horizontal flipping:The image has a horizontal rotation that affects the right and left sides. The components of $h\varpi$ and h_L indicate the existing position of the pixel after horizontal y-axis reflection, and it is expressed as,

$$\begin{bmatrix} \hbar_{\varpi} \\ \hbar_L \end{bmatrix} = \begin{bmatrix} -1 & 0 \\ 0 & 1 \end{bmatrix} \cdot \begin{bmatrix} \varpi \\ L \end{bmatrix} \tag{4}$$

Horizontal and Vertical flipping:Since the image alternated between a vertical and a horizontal column, both of the columns are endangered. Moreover, $h\varpi$ and h_L denotes present coordinates of each pixel after flipping vertical and horizontal axes. It is articulated as

$$\begin{bmatrix} \hbar_{\varpi} \\ \hbar_{L} \end{bmatrix} = \begin{bmatrix} -1 & 0 \\ 0 & -1 \end{bmatrix} \cdot \begin{bmatrix} \varpi \\ L \end{bmatrix} \quad (5)$$

Furthermore, the consequence image after flipping is specified as Υ_{a1} .

ii).Rotation: Rotation is accomplished by rotating images around a left- or right-pointing axis at an angle between 1 and 360. It is employed to produce images that vary from the actual image by a certain angle degree in a cumulative way. The rotation feature is demonstrated as,

$$\begin{bmatrix} \hbar_{\varpi} \\ \hbar_{L} \end{bmatrix} = \begin{bmatrix} \cos\phi & -\sin\phi \\ \sin\phi & \cos\phi \end{bmatrix} \cdot \begin{bmatrix} \varpi \\ L \end{bmatrix} \quad (6)$$

In this case, formed result after rotation is signified by Υ_{a2} .

iii.) Scaling: The particular image dimension and size are chosen throughout scaling process. The training set is also improved by employing the updated version of the data. The image after scaling is stated as Υ_{a3} .

iv.) Color augmentation: By changing values, the pixel values are modified directly, thereby altering the color property of image. Brightness, grayscale, hue, contrast and saturation modifications are made to attain color augmentation. In this case, augmented image is denoted as Υ_{a4} . Consequently, a process of image augmentation is demonstrated as

$$\Upsilon_{a} = \{\Upsilon_{a1}, \Upsilon_{a2}, \Upsilon_{a3}, \Upsilon_{a4}\} \quad (7)$$

e). Feature extraction

It helps reduce the quantity of irrelevant data in the dataset by identifying the important properties of the data. The augmented image Υ a are used as input to create the selected features for the processes which are explained in further sections. Moreover, statistical features, CNN, GLCM, CLBP, DWT, PHoG, LVP and LGXP are also mined. The Υ_{a} is taken as the input for feature extraction

i.Statistical features

Mean, median, standard deviation, variance, skewness and kurtosis are the statistical features12,24,25 considered in this section. The algebraic relation of statistical features is specified as follows.

Mean: The sum of all the pixel values in an image is divided by the total number of pixels in the image gives the mean12 of the image.

$$g_1 = \left(\frac{1}{c \times \varepsilon}\right) \sum_{w=0}^{c-1} \sum_{u=0}^{\varepsilon-1} h(w,u) \tag{8}$$

Here, mean is denoted as g_1 , size of image is represented as $c \times \varepsilon$, pixel location is indicated as w,u, and pixel intensity is denoted as h (w ,u) .

Median:The median25 is the number dividing the higher half of a data sample or population from the lower half. The data are arranged from least value to greatest value, and middle value is used to calculate the median of the Red (R) and Green (G) pixels intensity ratio values. Moreover, median is denoted by the term g_2 .

Standard deviation**:**The standard deviation12 is a measure of in homogeneity and the second central moment representing the probability distribution of an observed population. A greater number denotes a superior intensity level and strong edge contrast in an image.

$$g_3 = \sqrt{\left(\frac{1}{c \times \varepsilon}\right) \sum_{w=0}^{c-1} \sum_{u=0}^{\varepsilon-1} \left(h(w,u) - G\right)^2} \tag{9}$$

Here, standard deviation is signified as g_3 .

Variance: The rate of allocation in gray levels is specified by variance, which is another element of an image. [24] In this situation, the variance increased as well if there was a variation in mean-based gray level amount. The variance value indicates deviation of every pixel from mean.

$$g_4 = \left(\frac{1}{c \times \varepsilon}\right) \sum_{w=0}^{c-1} \sum_{u=0}^{\varepsilon-1} \left(h(w,u) - G\right)^2 \tag{10}$$

where, variance is denoted as g_4 .

Skewness: A metric for symmetry or lack of symmetry is called as skewness. [12] The skewness of random variable $g_5(\lambda)$, which is expressed below,

$$g_5(\lambda) = \left(\frac{1}{c \times \varepsilon}\right) \frac{\Sigma (h(w,u) - G)^3 |}{(g_3)^3} \tag{11}$$

where in, skewness is represented by the term g_5

Kurtosis: The parameter known as Kurtosis12 describes the shape of the probability distribution of a random variable.

$$g_6(\lambda) = \left(\frac{1}{c \times \varepsilon}\right) \frac{\Sigma (h(w,u) - G)^4 |}{(g_3)^4} \tag{12}$$

where, random variable is represented as λ , and kurtosis is denoted by g_6 .

ii. CNN features

CNNs[13] are artificial neural networks that are deep and feed-forward. Convolutional, pooling, and fully connected layers are three different categories of layers included in a conventional CNN. The objective of the convolution layer is to separate several feature representations from input. The pooling layers significantly contribute to the performance improvement of the model by reducing over-fitting, and computational cost. The inclusion of the features from previous convolutional layers is the main purpose of fully connected layers, which are described below. Local connectivity and shared weights are two significant techniques employed in CNNs that seek to optimize speed and minimize memory usage, feature generated from convolution layer is CNN feature and is designated as g_7 . In figure 3 illustrates the diagram for CNN features

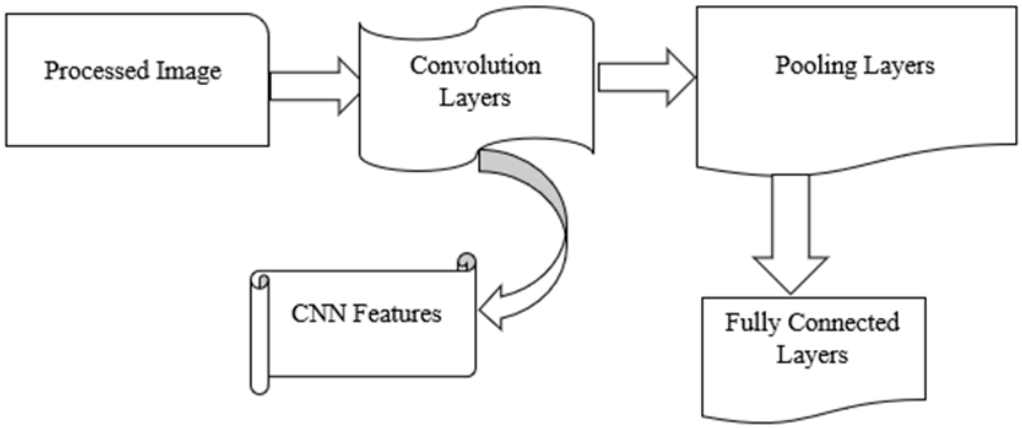

Figure 3. Schematic view of CNN Feature

iii. GLCM features

GLCM14 is a statistical technique for analyzing textures that considers the spatial relationship between the pixels. In this context, GLCM features like homogeneity, correlation, entropy, energy, and contrast are mined from augmented image Υ_a . The process is done briefly provided as follows, -

Energy: The significant number of repeating pixel combinations is known as energy. The affinity in an image is calculated using subsequent equation:

$$g_8 = \sqrt{\sum_{k=0}^{3-1}\sum_{r=0}^{\ell-1} h^2 * (k,r)} \qquad (13)$$

wherein, energy is represented as g_8 .

Contrast: The contrast gives the variation of the measurement of pixel intensities and their surrounding pixels, and is depicted as.

$$g_9 = \sum_{w=0}^{c-1}\sum_{u=0}^{\varepsilon-1} (w-u)^2 \, h(w,u) \qquad (14)$$

contrast is denoted as g_9.

Correlation: Correlation is the size of spatial features dependances between the pixels

$$g_{10} = \frac{\sum_{k=0}^{3-1}\sum_{r=0}^{\ell-1}(k,r)h(k,r) - F_k F_r}{\omega_k \omega_r} \quad (15)$$

correlation is indicated as g_{10}.

Homogeneity: The local consistency of an image is measured by homogeneity. It has one or more ranges of values to distinguish with non-textured and textured, and is also known as the "inverse difference moment."

$$g_{11} = \sum_{k=0}^{3-1}\sum_{r=0}^{\ell-1}\frac{1}{1+(k-r)^2}h(k,r) \quad (16)$$

homogeneity is signified as g_{11}.

Entropy: It is used to describe the randomness in augmented image and is stated as:

$$g_{12} = -\sum_{k=0}^{3-1}\sum_{r=0}^{\ell-1}h(k,r)\log_2 h(k,r) \quad (17)$$

grey scales are represented as k and r, translation factor and entropy is denoted as g_{12} .

iv). CLBP

The CLBP15 function is used to extract the local information from the augmented image Ƴa . It is used to characterize discriminatory information from the image and strengthen robustness of textural feature depiction. CLBP feature contemplates both symbols Ξ and magnitude Φ of local variances along with the value of center grey level υ . Moreover, CLBP feature consists of three features, such as CLBP _ Ξ , CLBP _ Φ , and CLBP _υ .

v).DWT

The most important feature extraction tool is DWT, 14 and it is used to fine-tune the wavelet coefficients from the images. An essential component of detection is the frequency data that the wavelet takes from a signal unit. In this case, images were mined from Low-Low (LL) sub-bands after being divided into spatial frequency units. Nevertheless, High-Low (HL) bands demonstrates higher performance than LL sub-bands.

vi).LGXP

The Local XOR pattern (LXP) operator and Gabor phase are both used by the LGXP descriptor. 18 The quantization of this descriptor into different levels of codes according to level of phases allows it to be used to encode Gabor stages. By using a behavioral model, the gathered Gabor stages are quantized.

vii). LVP

By estimating the distance between the target and surrounding pixels in various orientations and from various distances, the LVP feature17 creates a vector representation of all pixels. In this instance, the micro patterns are extracted from the paired vector orientation using the Comparative Space Transform (CST). Redundancy and length and are decreased by LVP function.

viii.) PHoG

A spatial shape descriptor called PHoG16 has been recently applied to the classification of images. The images are directed at various resolutions into the regions and spread over edge orientation inside the region. The HOG is displayed in the area of each image that corresponds to each resolution. A highly developed edge indicator then uses a grayscale image to classify PHOG feature, leading to the creation of a four-level dimensional pyramid. Nevertheless, HOG is noticed for each bin in each level and totaled to develop PHOG.

f. Leukemia classification using FMO-DenseNet model.

A highly common and dangerous cancer that begins in the tissues that produce blood is leukemia. Leukemia is categorized by examining at the chronic and acute disease development as well as its affected white blood cell rate. The blood cells are aberrant in acute leukemia and incapable of functioning normally. In this case, the leukemia classification is performed by utilizing FMO-DenseNet model. It is carried out by employing DenseNet, 19 which is tuned by proposed FMO. Here, feature vector Ψ is taken as input for leukemia classification.

i. Planning of DenseNet

DenseNet19 has a lot of dense connectivity when compared to other networks like Visual Geometry Group Network (VGGNet) and Residual Network (ResNet). DenseNet was chosen as the leukemia classification algorithm in this work because it effectively reduces vanishing gradient issue, enhances feature map circulation, and uses less parameters. DenseNet offers direct contacts from every layer to all succeeding layers, which can improve flow of information between layers

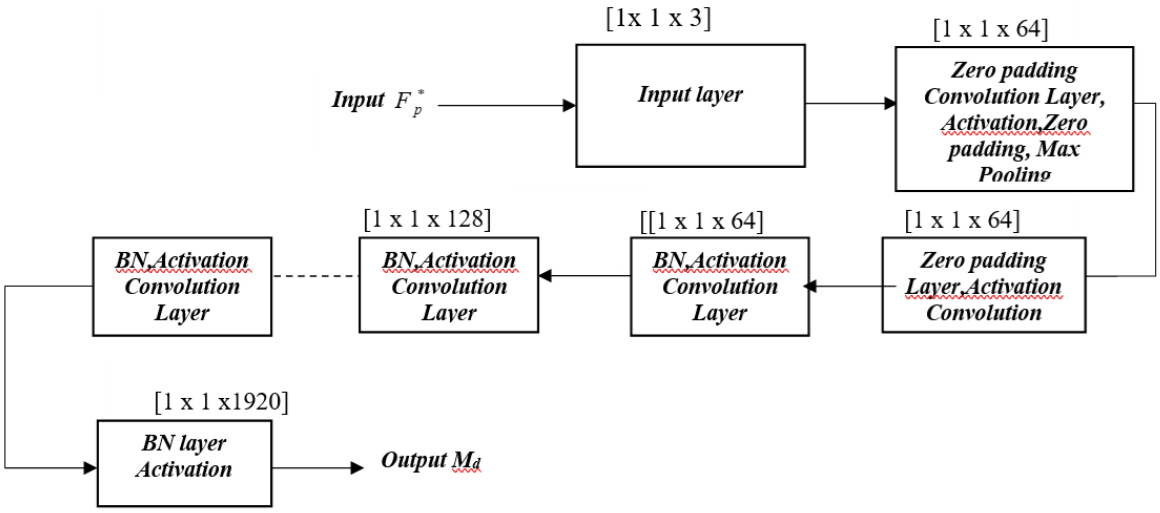

Figure 4. Architecture of DenseNet

ii. Training of DenseNet using proposed FMO

DenseNet is efficaciously trained to classify the areas of a leukemia using the FMO method, which combines FC21 and MA20 approaches. In particular, the social interactions and the mating rituals of mayflies serve as an inspiration for MA. 20 A potential solution to the issue is represented by each position of mayfly in search space. The male and female populations of mayflies are first represented by two randomly generated sets of mayflies. Every mayfly has a unique flying direction that is a dynamic mixture of its personal and social flying involvements, and a velocity of mayfly is termed as the change in its location. Each mayfly specifically modifies its trajectory to reach both the best position it has ever reached for itself and the entire swarm. This method improved exploration and shown outstanding convergence behavior, frequently arriving at the best overall solution in the first few iterations. Additionally, a fractional concept21 is employed to combined features before utilizing fractional calculus to arrange the features. Based on prior iterations, the FC is used to evaluate the optimal solution and is built to capture sequential information. The improvement boosts the effectiveness of both the proposed optimization technique and revised solution. Combining these two methods makes it feasible to tackle optimization difficulties with great results and a faster convergence rate. The algorithmic phases that comprise DenseNet training process are labeled as below

Step i): Initialization

Step ii): Estimating fitness function

Step iii): Movement of male mayflies

Step iv): Movement of female mayflies

Step v): Mating of mayflies

Step vi): Re-evaluating fitness

Step vii): Termination

Pseudocode of FMO is labeled in Table 1.The FMO algorithm is effective in generating the finest hyperparameters of the DenseNet, which is beneficial for classifying leukemia. The FMO algorithm generates global optima with minimum volume of complication by FC with regard to MA method.

Table 1.Pseudocode of proposed FMO
Initialize male and female mayfly population and velocity
Estimate solutions
Determine global best b^{best}
Do While stopping principles are not me
Apprise velocities and solutions of males and females
Assess solutions
Rank the mayflies
Mate the mayflies
Estimate offspring
Isolate offspring to male and female arbitrarily
Exchange worst solutions with best solutions
Apprise H^{best} and b^{best}
end while

2.3.2 Accumulation at the server

Once leukemia has been identified, the server aggregates weights derived from various local training data in data aggregation phase. At this point, the weights of local model are averaged to assess the weights of global model. The scheme holds X amount of local nodes ζ that produces weight ν s at every node an execute data aggregation ρ to calculate normal weight ℵ , which is demonstrated in figure 5.

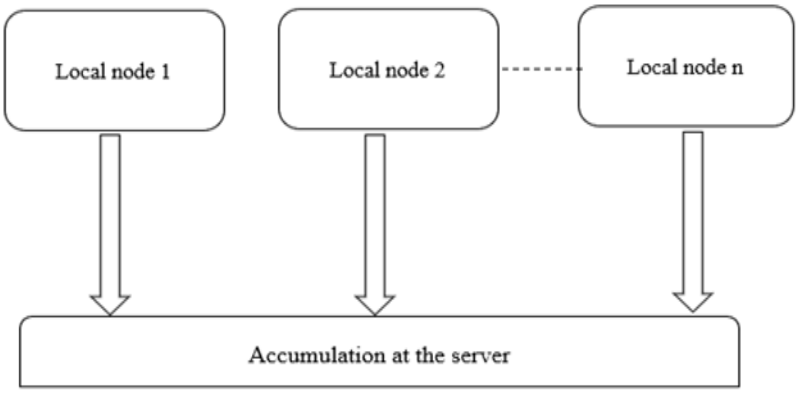

Figure 5. Data aggregation at the server

3.Results

The results of FMO-DenseNet in relation to the evaluation measures are elucidated in this section. The efficacy of introduced strategy is also revealed by comparing results of modeled technique with existing models.

3.1 Evaluation metrics

By using evaluation metrics, the effectiveness of the FMO-DenseNet is assessed. The measures used in this paper are accuracy, MSE, loss function, RMSE, TPR and TNR.

i) Accuracy: The ratio of blood smear images that are accurately categorized as either healthy or having leukaemia is determined by this metric.

ii) TPR: The sensitivity is the percentage of infected patients that are properly recognized as having leukemia. In this case, sensitivity is also called as TPR.

iii) TNR: TNR is also referred to as specificity, which measures the system by determining proportion of properly detected negative samples to all negative samples.

iv) MSE: MSE is a measure that merged the original and predicted dimensions.

v) RMSE: The square root of the squared error between the original and expected measures.

vi) Loss function: The distance between these detected values and the actual label values is indicated by loss function. The loss function also called as error function, that gives an excellent comprehension of prediction error.

3.2 Experimental results

The sample image outcomes for leukemia classification are showed in figure 6. Input blood smear image shows in figure 6a), pre-processed image is demonstrated in figure 6b), segmented image is deliberated in figure 6c). Moreover, figure 6d) and figure 6e) demonstrates CLBP extracted images and LGXP extracted from corresponding images.

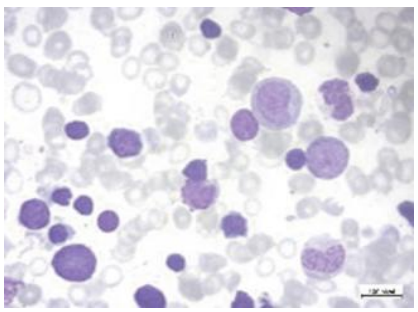

a)inputimage

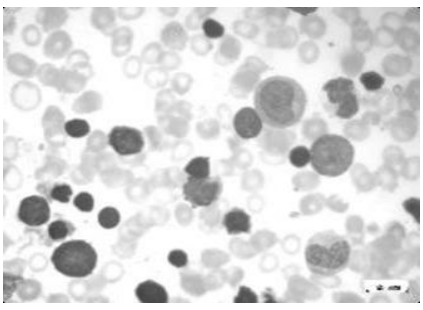

b) pre processed image

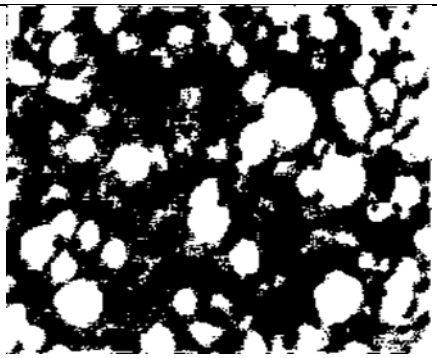

c) segmented image

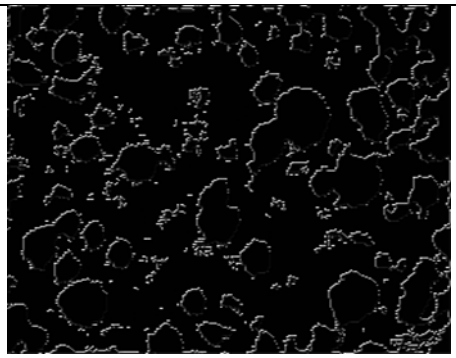

d) extracted CLBP image

Figure6. ExperimentaloutcomesofFMO-DenseNet, a) inputimage, b) pre processed image, c) segmented image, d) extracted CLBP image

3.2 Performance analysis

Below Figure 7a) reveals valuation of FMO-DenseNet utilizing accuracy. For time stamp of 50sec, the accuracy attained by proposed FMO-DenseNet with epoch 20, 40, 60, and 80 is 85.5%, 87.0%, 90.8% and 94.5%. Figure 7b) shows analysis of FMO-DenseNet with loss function. When time stamp is 50sec, the loss function calculated by FMO-DenseNet by considering the epoch as 20, 40, 60 and 80 is 14.5%, 13.0%, 9.2% and 5.5%. The performance assessment of FMO-DenseNet using MSE is displayed in figure 7c). With 50sec of time stamp, FMODenseNet attained MSE of 22.3%, 12.0%, 10.2% and 9.3%, corresponding to 20, 40, 60, and 80 epochs. Moreover, figure 7d) demonstrates RMSE-based valuation of FMO-DenseNet.The RMSE achieved by FMO-DenseNet with 50sec of time stamp is 4.73%, 34.6%, 32.0% and 30.4%, for 20, 40, 60, and 80 epochs. Figure 7e) shows the evaluation of FMO-DenseNet with respect to TNR. With 20, 40, 60, and 80 epochs, the TNR got by FMO-DenseNet is 87.7%, 90.2%, 93.8% and 96.9% for time stamp of 50sec. The evaluation of the FMODenseNet with TPR is shown in figure 7f). The FMO-DenseNet is found to have recorded TPR of 85.2%, 90.9%, 91.7% and 95.3% with 20, 40, 60, and 80 epochs, corresponding to time stamp of 50sec.

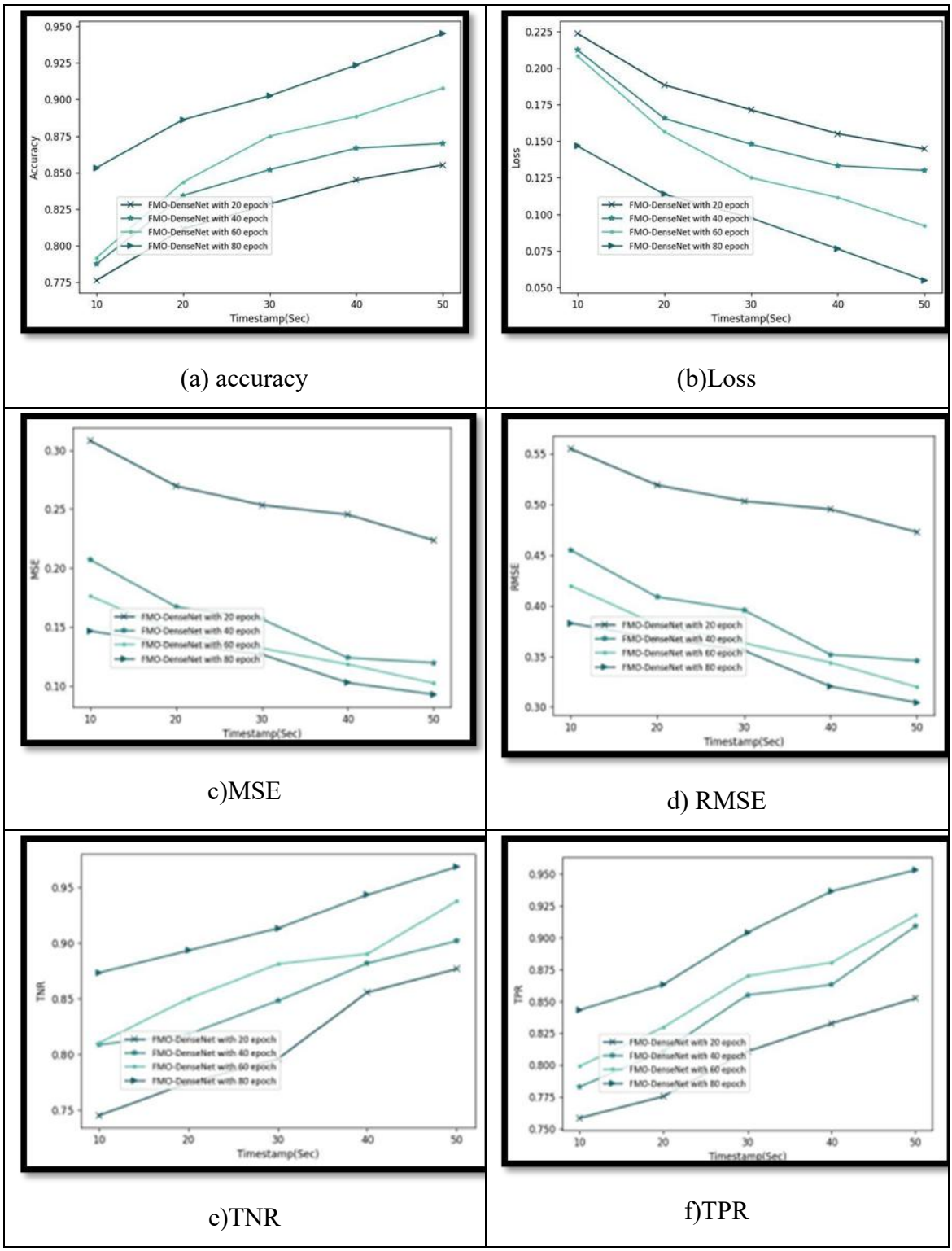

Figure7. Performance analysis of FMO- DenseNet, a) accuracy ,b) loss function, c)MSE, d) RMSE, e) TNR, f) TPR

3.4 Comparative methods

The FMO-DenseNet is compared with methods, such as CNN, 1 inception v3 XGBoost, 2 DNN, 3 and ResNet-504 in order to authenticate the supremacy of the DenseNet.

3.5 Comparative analysis

Below Figure 8 investigates FMO-DenseNet performance while assessing different time stamp. Accuracy-based assessment of FMO-DenseNet is displayed in figure 8a). By considering time stamp is 50sec, accuracy computed the methods like CNN, inception v3 XGBoost, DNN, and ResNet-50 is 84.3%, 88.7%, 89.5%, 90.2% and 94.3%. This validates that difference produced by FMO-DenseNet is 10.60%, 5.94%, 5.09%, and 4.35%. Similarly, figure 8b) shows loss function-based assessment of FMO-DenseNet. For the prevailing approaches, like CNN, inception v3 XGBoost, DNN, and ResNet-50, the loss function valueis 15.7%, 11.3%, 10.5%, 9.5%, and 5.7%, correspondingly, with time stamp of 50sec. Figure 8c) demonstrates MSE-based valuation of FMO-DenseNet. With 50sec of time stamp, FMODenseNet calculated a MSE value of 9.2%, while CNN, inception v3 XGBoost, DNN, and ResNet-50 attained values are 22.6%, 15%, 13.7%, and 11.8%. The estimation of FMO-DenseNet based on RMSE is revealed in figure 8d). When considering time stamp of 50sec, the FMO-DenseNet achieved RMSE value of 30.4% when compared to RMSE values of 47.5% for CNN, 38.8% for inception v3 XGBoost, 37.1% for DNN, and 34.4% for ResNet50. The FMO-DenseNet with TNR analysis is illustrated in figure 8e). By considering time stamp as 50sec, TNR of FMO-DenseNet is computed at 96.5%, which is superior than TNR of CNN, inception v3 XGBoost, DNN, and ResNet-50 of as 86.8%, 87.8%, 91.3%, and 84.1%, correspondingly. This shows performance enhancement of FMO-DenseNet is 10.05%, 9.02%, 5.39%, and 12.85%. Also, figure 8f) displays TPR based assessment of FMO-DenseNet. According to existing approaches like CNN, inception v3 XGBoost, DNN, ResNet-50 and FMO-DenseNet, the TPR value is 86%, 84.7%, 88.8%, 91.9%, and 95.3%, with time stamp of 50sec. This shows that FMO-DenseNet produces high variations of 9.76%, 11.12%, 6.82%, and 3.57%.

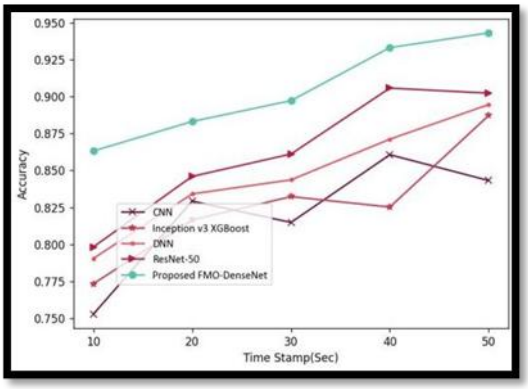

a)accuracy

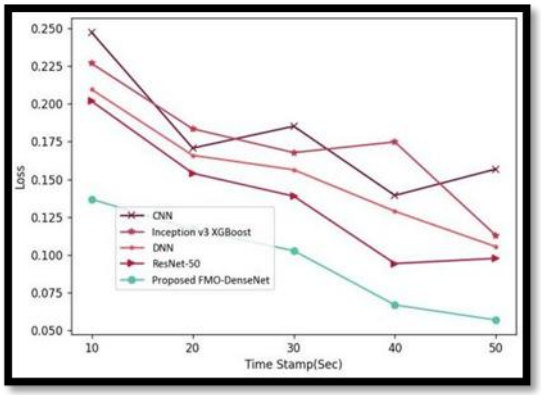

b)lossfunction

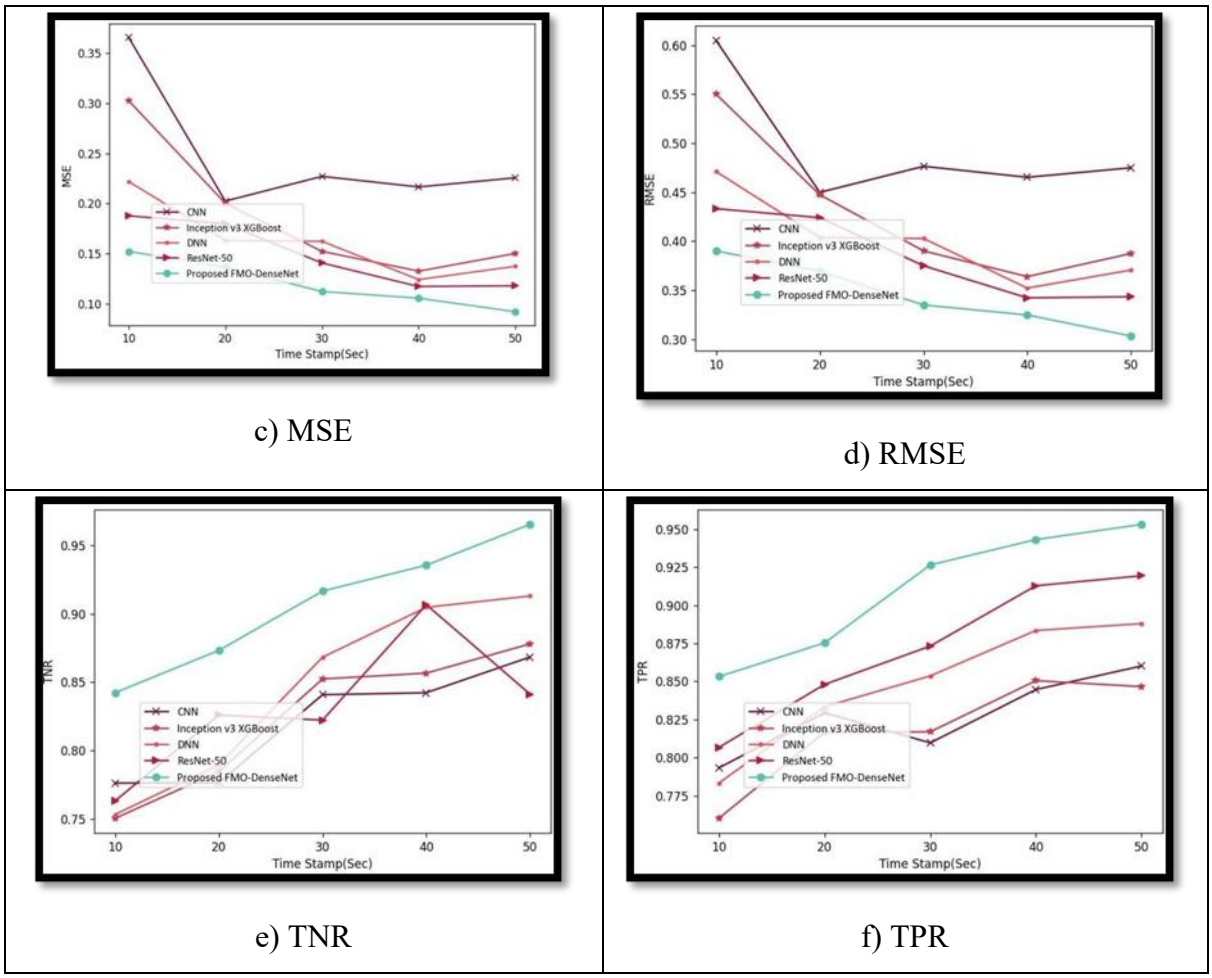

c) MSE

d) RMSE

e) TNR

f) TPR

Figure 8. Comparative analysis of FMO-Dense Net, a) accuracy, b) loss function, c) MSE, d) RMSE, e) TNR, f) TNR

4. Discussion

4.1 Comparative discussion

Relative discussion of FMO-DenseNet established in this work for classifying leukemia. Table 1 demonstrates the values of accuracy, loss function, MSE, RMSE, TNR and TPR noted by the various methods revised in literature together with the proposed technique. With the time stamp of 50sec, the values attained in the table are presented. The proposed FMO-DenseNet gained superior accuracy of 94.3%, whereas the existing approaches including CNN, inception v3 XGBoost, DNN, ResNet-50 and FMODenseNet calculated accuracy of 84.3%, 88.7%, 89.5%, and 90.2%. Moreover, loss function is computed by CNN is 15.7%, inception v3 XGBoost is 11.3%, DNN is 10.5% and ResNet50 is 9.5%, whereas minimum loss function attained by FMO-DenseNet is 5.7%.Additionally, the MSE values obtained from existing techniques like CNN, inception v3 XGBoost, DNN, ResNet-50 are 22.6%, 15%, 13.7%, and

11.8% whereas FMO-DenseNet gained minimum MSE is 9.2%. The RMSE values achieved by FMO-DenseNet is 30.4%, while RMSE measured by CNN is 47.5%, inception v3 XGBoost is 38.8%, DNN is 37.1% and ResNet-50 is 34.4% respectively. Furthermore, the maximum TNR of FMO-DenseNet computed at 96.5%, whereas TNR measured is 86.8% for CNN, 87.8% for inception v3 XGBoost, 91.3% for DNN, and 84.1% for ResNet-50. Similarly, CNN, inception v3 XGBoost, DNN, ResNet-50 and FMO-DenseNet obtained TPR of 86%, 84.7%, 88.8%, 91.9%, and 95.3%.The FMO-DenseNet method offers well performance than other methods stated here.DenseNet model is utilized for leukemia classification and effectively capture significant feature data of leukemia thus providing superior performance during classification process. By combining FL with DenseNet model during classification process, the classes that severely affected network performance are accurately identified while preserving the data privacy.

Table 1. Comparative discussion of proposed FMO-DenseNet

Metrics/ Methods	**CNN**	**inception v3 XGBoost**	**DNN**	**ResNet- 50**	**Proposed FMO-DenseNet**
Loss function (%)	15.70	11.30	10.50	9.50	**5.70**
TPR (%)	86.0	84.70	88.80	91.90	**95.30**
TNR(%)	86.80	87.80	91.30	84.10	**96.50**
MSE (%)	22.60	15.0	13.70	11.80	**9.20**
RMSE (%)	30.40	47.50	38.80	37.10	**34.40**
Accuracy(%)	84.30	88.70	89.50	90.20	**94.30**

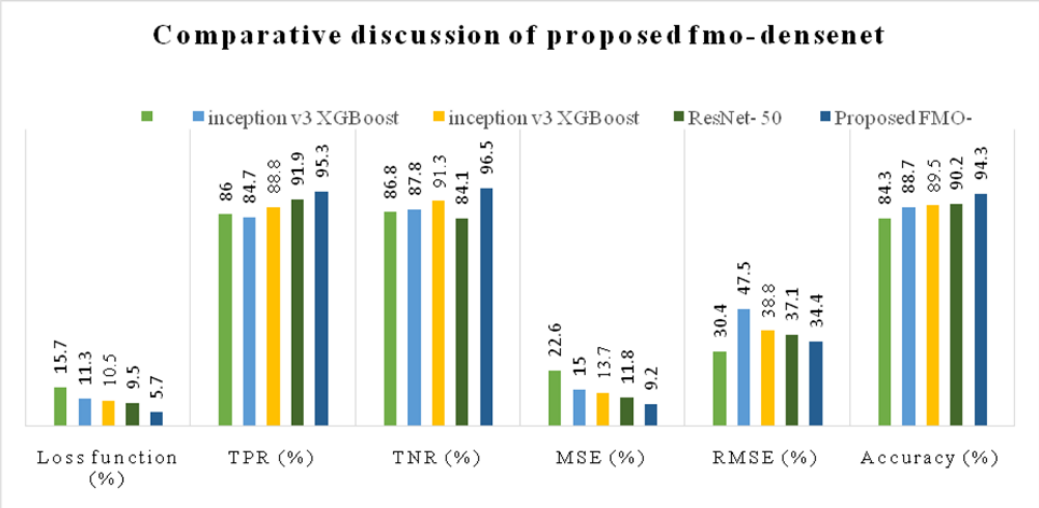

Figure 9. Comparative discussion of proposed FMO-DenseNet

5. Conclusion

In this work a competent approach for classifying leukemia employing the FMO-DenseNet that has been proposed utilizing FL. The process accomplished in the training model are follows. From the ALL database, input image is taken and send to further pre-processing. Here, AMF is used as part of pre-processing. Cell segmentation is done using scribble2label after the image has been pre-processed. Moreover, data augmentation is performed by utilizing flipping, color augmentation, scaling and rotation. Subsequently, feature extraction is executed utilizing several features such as CLBP, PHoG, LVP, DWT, LGXP, CNN features, statistical features of mean, kurtosis, median, variance, standard deviation, skewness and GLCM features include correlation, entropy, homogeneity, contrast, energy. Furthermore, the classification of leukemia is carried out by using DenseNet, which is tuned by proposed FMO. The FMO model is the amalgamation of MA and FC. The results showed that FMO-DenseNet attained maximum accuracy, TNR and TPR of 94.3%, 96.5% and 95.3% respectively. Moreover, FMO-DenseNet gained minimum loss function, MSE and RMSE of 5.7%, 9.2% and 34.4%. In the future, the hybrid neural network-based model will be implemented and the performance of model could be further enhanced by using large databases.

6. Declarations

Funding No funding was obtained for this study.

Conflict of Interest The authors declare that there are no conflicts of interest regarding the publication of this article.

Ethics approval This article contains no studies with human participants or animals performed by any of the authors.

Data Availability statement

Availability of data and materials

Blood Cells Cancer (ALL) dataset was taken from“https://www.kaggle.com/datasets/mohammadamireshraghi/blood-cell-cancer-all-4class”, accessed on October, 2023. BraTS 2020 Dataset, https://www.med.upenn.edu/cbica/brats2020/ accessed February 2024.

References

[1] Zakir Ullah M, Zheng Y, Song J, Aslam S, Xu C, Kiazolu GD, Wang L, An attentionbased convolutional neural network for acute lymphoblastic leukemia classification, Applied Sciences 11:10662, 2021.

[2] Ansari S, Navin AH, Sangar AB, Gharamaleki JV, Danishvar S, A customized efficient deep learning model for the diagnosis of acute leukemia cells based on lymphocyte and monocyte images, Electronics 12:322, 2023.

[3] Ramaneswaran S, Srinivasan K, Vincent PDR, Chang CY, Hybrid inception v3 XGBoost model for acute lymphoblastic leukemia classification, Computational and Mathematical Methods in Medicine 1-10, 2021.

[4] Sampathila N, Chadaga K, Goswami N, Chadaga RP, Pandya M, Prabhu S, Bairy MG, Katta SS, Bhat D, Upadya SP, Customized deep learning classifier for detection of acute lymphoblastic leukemia using blood smear images, In Healthcare 10:1812, 2022.

[5] Baig R, Rehman A, Almuhaimeed A, Alzahrani A, Rauf HT, Detecting malignant leukemia cells using microscopic blood smear images: a deep learning approach, Applied Sciences 12:6317, 2022.

[6] Sulaiman A, Kaur S, Gupta S, Alshahrani H, Reshan MSA, Alyami S, Shaikh A, ResRandSVM: Hybrid Approach for Acute Lymphocytic Leukemia Classification in Blood Smear Images, Diagnostics 13:2121, 2023.

[7] Mallick PK, Mohapatra SK, Chae GS, Mohanty MN, Convergent learning–based model for leukemia classification from gene expression, Personal and Ubiquitous Computing 27:1103-1110, 2023.

[8] Diaz Resendiz JL, Ponomaryov V, Reyes R, Sadovnychiy S, Explainable CAD System for Classification of Acute Lymphoblastic Leukemia Based on a Robust White Blood Cell Segmentation, Cancers 15:3376, 2023.

[9] Jayasudha S, Comparision of preprocess techniques for brain image using machine learning, Information Technology in Industry 9:653-656, 2021.

[10] Lee H, Jeong WK, Scribble2label: Scribble-supervised cell segmentation via selfgenerating pseudo-labels with consistency, In Medical Image Computing and Computer Assisted Intervention–MICCAI 2020: 23rd International Conference, Lima, Peru 14-23, 2020.

[11] Khalifa NE, Loey M, Mirjalili S, A comprehensive survey of recent trends in deep learning for digital images augmentation, Artificial Intelligence Review 1-27, 2022.

[12] Bahadure NB, Ray AK, Thethi HP, Image analysis for MRI based brain tumor detection and feature extraction using biologically inspired BWT and SVM, International journal of biomedical imaging 2017.

[13] Su R, Liu T, Sun C, Jin Q, Jennane R, Wei L, Fusing convolutional neural network features with hand-crafted features for osteoporosis diagnoses, Neuro computing 385:300- 309, 2020.

[14] Varuna Shree N, Kumar TNR, Identification and classification of brain tumor MRI images with feature extraction using DWT and probabilistic neural network, Brain informatics 5:23-30, 2018.

[15] Dar JA, Srivastava KK, Mishra A. Lung anomaly detection from respiratory sound database (sound signals). Comput Biol Med. 2023 Sep;164:107311. doi: 10.1016/j.compbiomed.2023.107311. Epub 2023 Aug 2. PMID: 37552916.

[16] Bai Y, Guo L, Jin L, Huang Q, A novel feature extraction method using pyramid histogram of orientation gradients for smile recognition, In 2009 16th IEEE International Conference on Image Processing (ICIP) 3305-3308, 2009.

[17] Fan KC, Hung TY, A novel local pattern descriptor—local vector pattern in high-order derivative space for face recognition, IEEE transactions on image processing 23:2877-2891, 2014.

[18] Kannan P, Shantha Selva Kumari R, VLSI architecture for LGXP texture for face recognition, Journal of Intelligent & Fuzzy Systems 27:2635-2647, 2014.

[19] Zhong Z, Zheng M, Mai H, Zhao J, Liu X, Cancer image classification based on DenseNet model, In Journal of physics: conference series 1651:012143, 2020.

[20] Zervoudakis K, Tsafarakis S, A mayfly optimization algorithm, Computers & Industrial Engineering 145:106559, 2020.

[21] Bhaladhare PR, Jinwala DC, A clustering approach for the-diversity model in privacy preserving data mining using fractional calculus-bacterial foraging optimization algorithm, Advances in Computer Engineering 2014.

[22] Suhila VM, Kovoor BC, Optimized hybrid approach for topic search using log likelihood and RV coefficient, In 2017 International Conference on Energy, Communication, Data Analytics and Soft Computing (ICECDS) 338-341, 2017.

[23] Roth HR, Chang K, Singh P, Neumark N, Li W, Gupta V, Gupta S, Qu L, Ihsani A, Bizzo BC, Wen Y, Federated learning for breast density classification: A real-world implementation, In Domain Adaptation and Representation Transfer, and Distributed and Collaborative Learning: Second MICCAI Workshop, DART 2020, and First

MICCAI Workshop, DCL 2020, Held in Conjunction with MICCAI 2020, Lima, Peru 181-191, 2020.

[24] Khairandish MO, Sharma M, Jain V, Chatterjee JM, Jhanjhi NZ, A hybrid CNN-SVM threshold segmentation approach for tumor detection and classification of MRI brain images, Irbm 43:290-299, 2022.

[25] Ghosh T, Bashar SK, Alam MS, Wahid K, Fattah SA, A statistical feature based novel method to detect bleeding in wireless capsule endoscopy images, In 2014 International Conference on Informatics, Electronics & Vision (ICIEV) 1-4, 2014.

[26] Srivastava, K., & Pal, A. Removal of A Smoke Region Using Maan Iteration Coupled with Cloud Computing.

[27] Konečný J, McMahan HB, Yu FX, Richtárik P, Suresh AT, Bacon D, Federated learning: Strategies for improving communication efficiency, arXiv preprint arXiv:1610.05492 2016.

[28] Goutam D, Sailaja S, Classification of acute myelogenous leukemia in blood microscopic images using supervised classifier, In 2015 IEEE International Conference on Engineering and Technology (ICETECH) 1-5, 2015.

[29] Boldú L, Merino A, Acevedo A, Molina A, Rodellar J, A deep learning model (ALNet) for the diagnosis of acute leukaemia lineage using peripheral blood cell images, Computer Methods and Programs in Biomedicine 202:105999, 2021.

[30] Brereton M, De La Salle B, Ardern J, Hyde K, Burthem J, Do we know why we make errors in morphological diagnosis? An analysis of approach and decision-making in haematological morphology, EBioMedicine 2:1224-1234, 2015.

[31] Lilhore UK, Poongodi M, Kaur A, Simaiya S, Algarni AD, Elmannai H, Vijayakumar V, Tunze GB, Hamdi M, Hybrid model for detection of cervical cancer using causal analysis and machine learning techniques, Computational and Mathematical Methods in Medicine 2022.

[32] Sermanet P, Eigen D, Zhang X, Mathieu M, Fergus R, LeCun Y, Overfeat: Integrated recognition, localization and detection using convolutional networks, arXiv preprint arXiv:1312.6229 2013.

[33] Dar, J.A., Srivastava, K.K. & Lone, S.A. Fr-WCSO- DRN: Fractional Water Cycle Swarm Optimizer-Based Deep Residual Network for Pulmonary Abnormality Detection from Respiratory Sound Signals. SN COMPUT. SCI. 3, 378 (2022). https://doi.org/10.1007/s42979-022-01264-0

[34] N. Dwivedi, K. Srivastava and N. Arya, "Sanskrit word recognition using Prewitt's operator and support vector classification," 2013 IEEE International Conference ON

Emerging Trends in Computing, Communication and Nanotechnology (ICECCN), Tirunelveli, India, 2013, pp. 265-269, doi: 10.1109/ICE-CCN.2013.6528506.

[35] Pal, A., Srivastava, K.K., Kumar, A. (2013). Parallel Character Reconstruction Expending Compute Unified Device Architecture. In: Meghanathan, N., Nagamalai, D., Chaki, N. (eds) Advances in Computing and Information Technology. Advances in Intelligent Systems and Computing, vol 177. Springer, Berlin, Heidelberg. https://doi.org/10.1007/978-3-642-31552-7_64

[36] Srivastava, K., & Kumar, A. (2011). A new approach of cloud: Computing infrastructure on demand. Trends in Information Management, 7(2).

Citation: Lila Misra, Rahul Shrivastava. (2025). Leukemia Classification Using an Optimized Hybrid Model: CNN, Resnet, DNN, And XGBOOST in Perspective. International Journal of Computer Engineering and Technology (IJCET), 16(3), 607–635.

Abstract Link: https://iaeme.com/Home/article_id/IJCET_16_03_037

Article Link:
https://iaeme.com/MasterAdmin/Journal_uploads/IJCET/VOLUME_16_ISSUE_3/IJCET_16_03_037.pdf

✉ **editor@iaeme.com**